

Rupture of DNA Aptamer: new insights from simulations

Rakesh Kumar Mishra,¹ Shesh Nath,¹ and Sanjay Kumar¹

*Department of Physics, Banaras Hindu University, Varanasi 221 005,
India*

Base-pockets (non-complementary base-pairs) in a double-stranded DNA play a crucial role in biological processes. Because of thermal fluctuations, it can lower the stability of DNA, whereas, in case of DNA aptamer, small molecules e.g. adenosinemonophosphate(AMP), adenosinetriphosphate(ATP) etc, form additional hydrogen bonds with base-pockets termed as “binding-pockets”, which enhance the stability. Using the Langevin Dynamics simulations of coarse grained model of DNA followed by atomistic simulations, we investigated the influence of base-pocket and binding-pocket on the stability of DNA aptamer. Striking differences have been reported here for the separation induced by temperature and force, which require further investigation by single molecule experiments.

I. INTRODUCTION

Aptamers are Guanine(G)-rich short oligonucleic acids (DNA, RNA), which can perform specific function^{1,2}. These have been developed *in vitro* through SELEX (Systematic Evolution of Ligands by Exponential Enrichment) process for better understanding of the behavior of antibodies, which are produced *in vivo* or in living cells¹⁻³. One of the most extensively characterized examples of aptamer is found in telomerase at the ends of eukaryotic chromosomes, where it plays an important role in gene regulation^{4,5}. DNA loops or base-pockets consisting of Guanine can interact with small molecules and proteins and thus enhance their stability, affinity and specificity⁶. For example, adenosinemonophosphate (AMP) binds to DNA loop (termed as binding-pocket) with eight hydrogen bonds, that increases the stability⁷⁻⁹ of aptamer. It served as the target of drugs for cancer treatment¹⁰. Their high affinity and selectivity with target proteins make them ideal and powerful probes in biosensors and potent pharmaceuticals¹¹⁻²¹. Thus, understanding of the conformational stability of DNA aptamers before and after the release of drug molecule, and the influence of the binding of other molecules, are of crucial importance.

A double-stranded DNA (dsDNA) can be separated in two single-stranded DNA by increasing the temperature and the process is termed as DNA melting. Traditional spectroscopic techniques used e.g. fluorescence spectroscopy, *UV-vis* spectroscopy etc. usually provide average responses for molecular interactions²². Single molecule force spectroscopy (SMFS) techniques have emerged as valuable tools for measuring the molecular interactions on a single molecule level, and thus unprecedented information about the stability of biomolecules have been achieved. For example, DNA rupture induced by SMFS techniques have been used to understand the strength of hydrogen bonds in nucleic acids, ligands-nucleic interaction, protein-DNA interactions etc.²³⁻²⁶. In DNA rupture all intact base-pairs break simultaneously and two strands get separated, when a force is applied either at 3' - 3' or 5' - 5' ends. This force is identified as rupture force. Motivated by these studies, attempts have recently been made to understand the enhanced stability of DNA aptamers²⁷⁻³¹. For

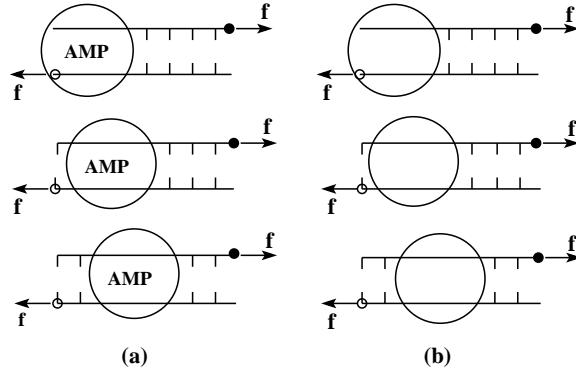


FIG. 1. Schematic representations of dsDNA under a shear force applied at the opposite ends with varying position of (a) binding-pocket (AMP), (b) base-pocket (without AMP). In the constant velocity simulation, one end marked by blank circle is kept fixed, while in the constant force simulation, the force is applied at both ends. The binding-pocket (AMP within circle) Fig. 1(a) corresponds to additional binding of hydrogen bonds with AMP. The circle in Fig. 1(b) represents the base-pocket consisting of G (say), where base-pairing is absent.

example, Nguyen et al.²⁷ measured the changes in rupture force of a DNA aptamer (that forms binding-pocket) with AMP (Fig. 1(a)) and without AMP (Fig. 1(b)), and thereby determined the dissociation constant at single-molecule level. Papamichael et al.²⁸ used an aptamer-coated probe and an IgE-coated mica surface to identify specific binding areas. Efforts have also been made to determine the rupture force of aptamer binding to proteins and cells, and it was revealed that the binding-pocket enhances the rupture force by many folds^{29–31}.

Despite the progress made, there are noticeable lack of investigations. For example, the melting of DNA aptamer in presence and absence of AMP and its dependence on the position in a DNA strand need to be measured and understood correctly. The aim of this paper is to develop a theoretical model to understand the role of a base-pocket and a binding-pocket on the rupture of a DNA aptamer. For this, a coarse grained model of DNA is developed. Here, dsDNA is made up of two segments. One of the segments consists of a DNA loop or the base-

pocket of eight G type nucleotides. The other segment is stem, which is made up of twelve G-C base-pairs. We vary the position of the binding-pocket (Fig. 1 (a)) and the base-pocket (Fig. 1(b)) along the chain, and measure the rupture force and melting temperature for both cases (with and without AMP). For the first time, we report the profile as a function of base/binding-pocket position. We find that even though the melting profile has one minima (U-shape), there are two minima (W-shape) for rupture. This reflects that there are two symmetric positions, where the system can be more unstable. Extensive atomistic simulations have been performed to validate these findings, which helped us to delineate the correct understanding of the role of base-pockets in the stability of DNA aptamer. In Sec. II, we briefly describe the model and the Langevin dynamics simulation to study the rupture of DNA aptamer^{32,33}. The discussion on the melting and rupture profile of DNA aptamer as a function of base/binding-pocket position has also been made in this section. In Sec. III, we briefly explain the atomistic simulation³⁴⁻³⁶ and discuss the model independency of the results. Finally in Sec. IV, we conclude with a discussion on some future perspectives.

II. MODEL AND METHOD

We first adopt a minimal model introduced in Ref.³² for a homo-sequence of dsDNA consisting of N base-pairs, where covalent bonds and base-pairing interactions are modelled by harmonic springs and Lennard-Jones (LJ) potentials, respectively. By using Langevin dynamics simulation, it was shown that the rupture force and the melting temperature remain qualitatively similar to the experiments²³⁻²⁶. Energy of the model system^{32,37,38} is given by.

$$\begin{aligned}
 E = & \sum_{l=1}^2 \sum_{j=1}^N k(\mathbf{r}_{j+1,j}^{(l)} - d_0)^2 + \sum_{l=1}^2 \sum_{i=1}^{N-2} \sum_{j>i+1}^N 4 \left(\frac{C}{|\mathbf{r}_{i,j}^{(l)}|^{12}} \right) \\
 & + \sum_{i=1}^N \sum_{j=1}^N 4\epsilon \left(\frac{C}{(|\mathbf{r}_i^{(1)} - \mathbf{r}_j^{(2)}|)^{12}} - \frac{A}{(|\mathbf{r}_i^{(1)} - \mathbf{r}_j^{(2)}|)^6} \delta_{ij} \right), \quad (1)
 \end{aligned}$$

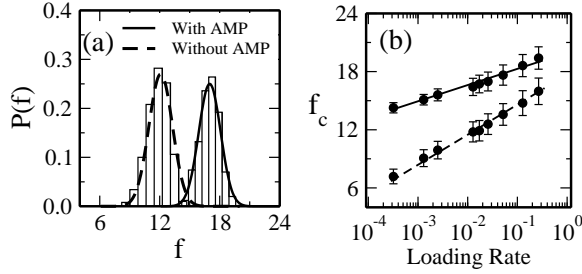


FIG. 2. (a) Probability distribution of rupture force of DNA aptamer with AMP (solid line) and without AMP (dashed line) for the same loading rate (0.0205). (b) Variation of rupture force with loading rate.

where N is the number of beads in each strand. Here, $\mathbf{r}_j^{(l)}$ represents the position of bead j on strand l . In the present case, $l = 1(2)$ corresponds to first (complementary) strand of dsDNA. The distance between intra-strand beads, $\mathbf{r}_{i,j}^{(l)}$, is defined as $|\mathbf{r}_i^{(l)} - \mathbf{r}_j^{(l)}|$. The harmonic (first) term with spring constant $k = 100$ couples the adjacent beads along each strand. The parameter $d_0 (= 1.12)$ corresponds to the equilibrium distance in the harmonic potential, which is close to the equilibrium position of the LJ potential. The second term takes care of excluded volume effects *i.e.*, two beads can not occupy the same space³⁹. The third term, described by the Lennard-Jones (LJ) potential, takes care of the mutual interaction between the two strands. The first term of LJ potential (same as second term of Eq.1) will not allow the overlap of two strands. The second term of the LJ potential corresponds to the base-pairing between two strands. The base-pairing interaction is restricted to the native contacts ($\delta_{ij} = 1$) only *i.e.*, the i^{th} base of the 1^{st} strand forms pair with the i^{th} base of the 2^{nd} strand only. It is to be noted here that ϵ represents the strength of the LJ potential. In Eq. 1, we use dimensionless distances and energy parameters and set $\epsilon = 1$, $C = 1$ and $A = 1$, which corresponds to a homosequence dsDNA. The binding-pocket and base-pocket can be modelled by substituting $A = 1$ & $\epsilon = 2$ (Fig. 1(a)) and $A = 0$ & $\epsilon = 1$ (Fig. 1(b)), respectively, among the bases inside the circle. The equation of motion is obtained from the following Langevin equation:

$$m \frac{d^2 \mathbf{r}}{dt^2} = -\zeta \frac{d\mathbf{r}}{dt} + \mathbf{F}_c(\mathbf{t}) + \mathbf{\Gamma}(\mathbf{t}), \quad (2)$$

where $m(= 1)$ and $\zeta(= 0.4)$ are the mass of a bead and the friction coefficient, respectively. Here, \mathbf{F}_c is defined as $-\frac{dE}{d\mathbf{r}}$ and the random force $\mathbf{\Gamma}$ is a white noise³⁸, i.e., $\langle \mathbf{\Gamma}(t)\mathbf{\Gamma}(t') \rangle = 6\zeta T \delta(t - t')$. The 6th order predictor-corrector algorithm with time step $\delta t=0.025$ has been used to integrate the equation of motion. The results are averaged over many trajectories.

First, we have calculated the rupture force of a dsDNA of two different lengths⁴⁰. We have inserted a base-pocket in the interior of the chain (circle in Fig. 1(b) and calculated the required force for the rupture at temperature $T = 0.12$. In order to obtain the rupture force for the DNA aptamer, we switched on the interaction among the base-pocket nucleotides with AMP (Fig. 1(a)): each of these extra interaction strength is double of the base-pairing interactions. Following the experimental protocol²⁷, we performed constant velocity simulation^{37,38} by fixing one end of a DNA strand marked by a blank circle in Fig. 1. Force $f = K(vt - x)$ is applied on the other end of the strand marked by filled circle in Fig. 1. Here, x is the displacement of the pulled monomer from its original position, v is the velocity, t is the time and $K(= 0.8)$ is the spring constant⁴¹. The rupture force is identified as the maximum force, at which two strands separate suddenly. A selection of rupture force distribution of 500 events have been shown in Fig. 2(a). For a given loading rate, the most probable rupture force f_c is obtained by the Gaussian fit of the distribution of rupture force²⁴. In Fig. 2(b), we have shown the variation of f_c (with and without AMP) with the loading rate (Kv). It is apparent from the plots that the rupture force required for the DNA aptamer is larger than the DNA (without AMP) with base-pocket, and the qualitative nature remains same as seen in the experiment²⁷.

For the better understanding of the role of base-pocket and binding-pocket, we varied its position along the chain continuously from one end to the other, and calculated the melting temperature (T_m) and rupture force (f_c) for each position in the constant force ensemble (CFE)³². The melting temperature is obtained here by monitoring the energy fluctuation

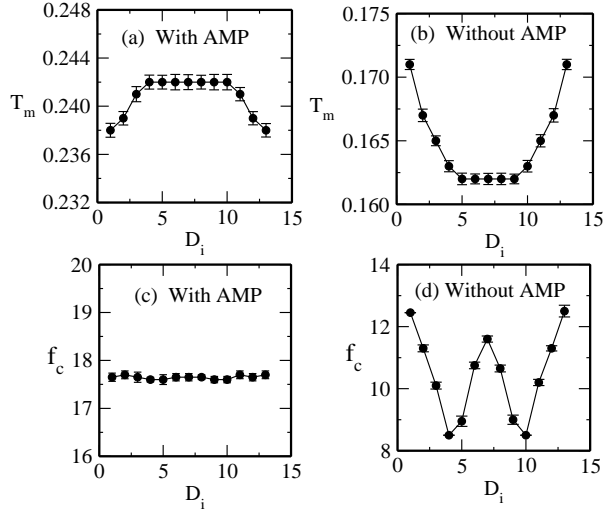


FIG. 3. (a) Variation of T_m with binding-pocket positions and (b) with base-pocket positions. (c) Variation of f_c with binding-pocket positions and (d) with base-pocket positions.

(ΔE) or the specific heat (C) with temperature, which are given by the following relations⁴²

$$\langle \Delta E \rangle = \langle E^2 \rangle - \langle E \rangle^2 \quad (3)$$

$$C = \frac{\langle \Delta E \rangle}{T^2}. \quad (4)$$

The peak in the specific heat curve gives the melting temperature. Since this simulation is in the equilibrium, we have used 10 realizations with different seeds and reported the mean value of the rupture force. In Fig.3 (a)–(d), we have plotted the variation of T_m (at $f = 0$) and f_c ($T = 0.06$) much below T_m as a function of pocket position (D_i). It is interesting to note that for thermal melting, the variation looks like “ \cap shape” for the DNA aptamer (with AMP) shown in Fig.3(a), and for without AMP, profile has “U- shape” having one minima (Fig. 3(b)). The rupture force remains invariant with binding-pocket positions for AMP (Fig.3(c)), which is consistent with experiment²⁷. Interestingly, in the absence of AMP, the profile has “W-shape”, *i.e.*, with two minima (Fig.3(d)). Although, one may intuitively expect the shape of profiles to be symmetric for the homosequence. But it is not apparent, why does the profile has one minimum for the thermal melting and two minima for the DNA rupture in the absence of AMP.

We now confine ourselves to understand these issues. In case of DNA aptamer melting, one would expect naively that the aptamer is more stable, when the binding-pocket is in the interior of the chain. Thus, T_m should be high (Fig. 3(a)) compare to the binding pocket at the end resulting in a “ \cap shape” profile. In absence of AMP, the profile looks like “U-shape”. For a short chain, DNA melting is well described by the two state model⁴³ with $\Delta G = \Delta H - T\Delta S$, where H and S are the enthalpy and entropy, respectively. The melting temperature $T_m = \frac{\Delta H}{\Delta S}$ corresponds to the state with $\Delta G = 0$ indicating that the system goes from the bound-state to the open-state and change in the free energy of the system is zero. It is often practically easier to identify T_m as the temperature where 50% hydrogen bonds are broken.

For a homo-sequence chain (without base-pocket), it was shown that the chain opens from the end rather than the interior of the chain⁴⁴. In such a case, the major contribution to the entropy comes from the opening of base-pairs near the end of the chain, and decreases to zero, when one approaches to the interior of the chain. In this case, there are two contributions to the entropy: entropy associated with opening of the end base-pairs (S_E) and the base-pocket entropy (S_{BP}). When a base-pocket is inserted at the end of DNA chain, there is an additional contribution to the entropy, which is greater than ΔS_E or (ΔS_{BP}), but less than the sum of two. Thus, T_m decreases to ~ 0.171 from ~ 0.181 ⁴⁰. As the base-pocket moves along the chain, entropy of interior base-pairs increases. Combined effect of both entropies reduces the melting temperature further. Once the base-pocket is deep inside, the total entropy of the system becomes equal to the sum of end-entropy and base-pocket entropy. As a result, T_m remains constant(~ 0.161) (Fig. 3(b)) irrespective of the base-pocket position. As base-pocket approaches towards the other end, by symmetry we observe “U-” shape profile. The conversion of reduced unit to real unit indicates that it is possible to observe it *in vitro*⁴⁵.

Understanding the decrease in T_m with base-pocket position does not explain, why the rupture profile of DNA has two minima. It is clear from the Fig. 3 (b) & (d) that the base-pocket entropy alone is not responsible for this (W) shape. Based on the ladder

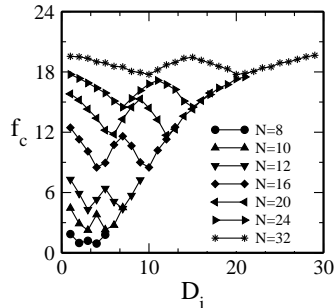


FIG. 4. Variation of f_c with base-pocket positions for different lengths.

model of DNA (homo-sequence), de Gennes proposed that the rupture force f_c is equal to $2f_1(\chi^{-1} \tanh(\chi \frac{N}{2}))^{47}$. Here, f_1 is the force required to separate a single base-pair and χ^{-1} is the de Gennes length, which is defined as $\sqrt{\frac{Q}{2R}}$. Q and R are the spring constants characteristic of stretching of the backbone and hydrogen bonds⁴⁷, respectively. de Gennes length is the length over which differential force is distributed. Above this length, the differential force approaches to zero and there is no extension in hydrogen bonds due to the applied force^{25,32}. When the base-pocket is at the end, four bases of one strand is under the tension, whereas the complementary four bases are free, thereby increasing the entropy of the system. The four bases act like a tethered length and a force is required to keep it stretched so that rupture can take place. It is nearly equal to the ruptured force of a 12 base-pair dsDNA with no defect. As the base-pocket moves towards the center, the entropy of base-pocket decreases as the ends of the base-pocket is now not free. Since, the de Gennes length for the base-pocket is infinite ($R = 0$), it implies that the differential force remains constant inside the base-pocket, thereby decreases the stability of DNA, and as a result, rupture force decreases further. The force acting at ends penetrates only up to the de Gennes length and within this, the rupture force keeps on decreasing as base-pocket moves and approaches to its minimum. Above a certain length, the rupture force starts increasing, which can be seen in Fig.3 (d) and approaches to the maximum at the middle of the chain. By symmetry, we get profile of two minima of “W-shape”.

It should be pointed here, that the de Gennes length in the present model is about ten⁴⁸,

but for a DNA of length 16 base-pairs (12 complementary and 4 non complementary), the minima is around $D_i = 4$. Note that the penetration depth for the two ends (say 5' - 5') is different because of the asymmetry arising due to the presence of base-pocket, and hence the minima shifts. If we increase the length of DNA, keeping the base-pocket size constant, one would then expect that the minima will shift towards 10 (above the de Gennes length, the end-effect vanishes). This indeed we see in Fig. 4, where the variation of f_c with base-pocket position for different chain lengths ($N = 8, 10, 12, 16, 20, 24$ and 32) has been plotted. In all cases, profiles have two minima, whereas minima shifts towards 10 as N increases. de Gennes equation predicts that f_c increases linearly with length for small values of N , and saturates at the higher values of N , which is consistent with recent experiment²⁵ and simulations³². Surprisingly, right side of the profile also appears to follow the de Gennes equation. This implies that, the base-pocket can reduce the effective length of the chain, so that the rupture force is less compare to the bulk value and approaches to a minimum value at a certain position. As the end-effect decreases, f_c starts increasing and approaches to its bulk value.

III. ATOMISTIC SIMULATION

In order to rule out the possibility that the above effect may be a consequence of the adopted model, we performed the atomistic simulations with explicit solvent. Here, we have taken homo-sequence DNA consisting of 12 G-C bps and a varying base-pocket of 8 G-nucleotides^{34-36,49}. The starting structure of the DNA duplex sequence having the base-pocket is built using make-na server⁵⁰. We used AMBER10 software package³⁴ with all atom (ff99SB) force field³⁵ to carry the simulation. Using the LEaP module in AMBER, we add the AMP molecule (Fig. 5(a)) in the base-pocket and then the Na^+ (counterions) to neutralize the negative charges on phosphate backbone group of DNA structure (Fig. 5(b)). This neutralized DNA aptamer structure is immersed in water box using TIP3P model for water⁵¹. We have chosen the box dimension in such a way that the ruptured DNA aptamer

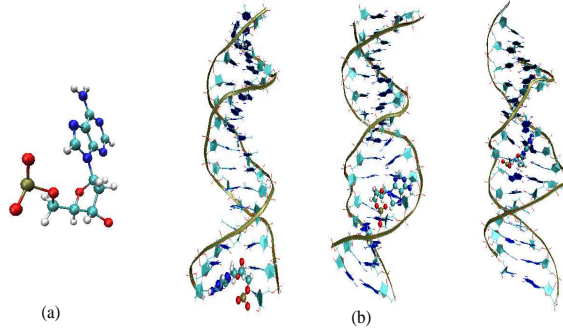


FIG. 5. (Color online) (a) Structure of AMP molecule, which has been inserted in the base-pocket. (b) Snapshots of binding of AMP molecule at three different positions ($D_i=1, 4$ and 7) in the DNA.

structure remains fully inside the water box. We have taken the box size of $57 \times 56 \times 183 \text{ \AA}^3$ which contains 15674 water molecules and 30 Na^+ (counterions). A force routine has been added in AMBER10 to do simulation at constant force^{49,52}. In this case, the force has been applied at $5' - 5'$ ends. The electrostatic interactions have been calculated with Particle Mesh Ewald (PME) method^{53,54} using a cubic B-spline interpolation of order 4 and a 10^{-5} tolerance is set for the direct space sum cut off. A real space cut off of 10 \AA is used for both the van der Waal and the electrostatic interactions. The system is equilibrated at $F = 0$ for 100 ps under a protocol described in Ref.^{55,56} and it has been ensured that AMP has bound with the base-pocket. We carried out simulations in the isothermal-isobaric (NPT) ensemble using a time step of 1 fs for 10 different realizations. We maintain the constant pressure by isotropic position scaling³⁴ with a reference pressure of 1 atm and a relaxation time of 2 ps. The constant temperature was maintained at 300 K using Langevin thermostat with a collision frequency of 1 ps^{-1} . We have used 3D periodic boundary conditions during the simulation.

Because of extensive time involved in the computation, we restricted ourselves at three different (extremum) base-pocket positions $D_i=1, 4$ and 7 (Fig. 5(b)) and calculated the rupture force with 10 realization of different seeds as a mean force. The required rupture forces for these positions are $840 \text{ pN} \pm 20 \text{ pN}$, $720 \text{ pN} \pm 20 \text{ pN}$ and $830 \text{ pN} \pm 20 \text{ pN}$,

indicating that the complete profile contains two minima⁵⁷. In presence of AMP, which interacts with the base-pocket, we find $f_c = 925\text{pN} \pm 20\text{pN}$ remains constant irrespective of binding-pocket position as seen earlier (Fig. 3(c)). This validates the finding of simple coarse grained model, which captured some essential but unexplored aspects of rupture mechanism of DNA aptamer.

IV. CONCLUSIONS

Our numerical studies clearly demonstrate that the force induced rupture and thermal melting of DNA aptamer will vary quite significantly. In melting, all the nucleotides get almost equal thermal knock from the solvent molecules, whereas in DNA rupture, force is applied at the ends and the differential force acts only up to the de Gennes length⁴⁷. As a result, the stability of DNA in presence of base-pocket is strikingly different (single minima *vs* double minima). This may have biological/pharmaceutical significance because after the release of drug molecule, the stability of carrier DNA depends on the position from which it is released. Hence, at this stage our studies warrant further investigations most likely by new experiments to explore the role of base-pockets and its position, which will significantly enhance our understanding about the stability of DNA aptamer and its suitability in the development and designing of drugs.

V. ACKNOWLEDGEMENTS

We thank G. Mishra, D. Giri and D. Dhar for many helpful discussions on the subject. We acknowledge financial supports from the DST, UGC and CSIR, New Delhi, India.

REFERENCES

- ¹C. Tuerk and L. Gold, Science **249**, 505 (1999).
- ²A. D. Ellington and J. W. Szostak, Nature **346**, 818 (1990).

- ³M.B. O'Donoghue, Xi. Shi, X. Fang and W. Tan, *Anal. Bioanal. Chem.* **402**, 3205 (2012).
- ⁴P. Sarkies, C. Reams, L. J. Simpson and J. E. Sale, *Mol. Cell* **40**, 703 (2010).
- ⁵M. Bejugam *et al.*, *J. Am. Chem. Soc.* **129**, 12926 (2007).
- ⁶A. D. Keefe, S. Pai, and A. Ellington, *Nature Reviews Drug Discovery*, **9**, 537 (2010).
- ⁷C. H. Lin and D. J. Patel, *Chem. Biol.* **4**, 817 (1997).
- ⁸C. Teller, S. Shimron and I. Willner, *Anal. Chem.* **81**, 9114 (2009).
- ⁹S. Nonin-Lecomte, C. H. Lin and D. J. Patel, *Biophys. J.* **81**, 3422 (2001).
- ¹⁰D. J. Patel, A. T. Phan and V. Kuryavyi, *Nucleic Acids Res.* **35**, 7429 (2007).
- ¹¹B. A. Sullenger and E. Gilboa, *Nature* **418**, 252 (2002).
- ¹²F. Hoppe-Seyler and K. Butz, *J. Mol. Med.* **78**, 426 (2000).
- ¹³E. J. Cho, J. W. Lee and A. D. Ellington, *Annu. Rev. Ana. Chem.* **2**, 241 (2009).
- ¹⁴J. Chen, Z. Fang, P. Lie and L. Zeng, *Anal. Chem.* **84**, 6321 (2012).
- ¹⁵P. M. Yangyuoru, S. Dhakal, Z. Yu, D. Koirala, S. M. Mwangela and H. Mao, *Anal. Chem.* **84**, 5298 (2012).
- ¹⁶M. Zayats, Y. Huang, R. Gill, Chun-an Ma and I. Willner, *J. Am. Chem Soc.* **128**, 13666 (2006).
- ¹⁷X. Zuo, Y. Xiao and K. W. Plaxco, *J. Am. Chem Soc.* **131**, 6944 (2009).
- ¹⁸B. Olcay, H. S. Christopher, K. George and H. G. William, *MTNA* **2**, e107 (2013).
- ¹⁹H. Sun, X. Zhu, P. Y. Lu, R. R. Rosato, W. Tan, and Y. Zu, *MTNA* **3**, e182 (2014).
- ²⁰G. Zhu *et al.*, *PNAS* **110**, 7998 (2013).
- ²¹L. Li *et al.*, *PNAS* **111**, 17099 (2014).
- ²²R. Wartell and A. Benight, *Phys. Rep.* **126**, 67 (1985).
- ²³G. U. Lee, L. A. Chrisey and R. J. Colton, *Science* **266**, 771 (1994).
- ²⁴T. Strunz, K. Oroszlan, R. Schäfer and H. J. Güntherodt, *PNAS* **96**, 11277 (1999).
- ²⁵K. Hatch *et al.*, *Phys. Rev. E* **78**, 011920 (2008).
- ²⁶C. Danilowicz, *et al.*, *PNAS* **106**, 13196 (2009).
- ²⁷T-H Nguyen, L. J. Steinbock, H-J. Butt, M. Helm and R. Berger, *J. Am. Chem Soc.* **133**, 2025 (2011).

- ²⁸I. K. Papamichael, P. M. Kreuzer and G. Guilbault, *Sens. Actuators B* **121**, 178 (2007).
- ²⁹J. Zlatanova, M. S. Lindsay and H. S. Leuba, *Prog. Biophys. Mol. Biol.* **74**, 37 (2000).
- ³⁰J. P. Yu, Y. X. Jiang, X. Y. Ma, Y. Lin and X. H. Fang, *Chem. Asian J.* **2**, 284 (2007).
- ³¹Y. Jiang, C. Zhu, L. Ling, L. Wan, X. Fang and C. Bai, *Anal. Chem.* **75**, 2112 (2003).
- ³²R. K. Mishra, G. Mishra, M. S. Li and S. Kumar, *Phys. Rev. E* **84**, 032903 (2011).
- ³³A FORTRAN code is developed to study the dynamics of the system.
- ³⁴D. A. Case *et al.*, AMBER 10, University of California, San Francisco (2008).
- ³⁵Y. Duan *et al.*, *J. Comput. Chem.* **24**, 1999 (2003).
- ³⁶S. Nath, T. Modi, R. K. Mishra, D. Giri, B. P. Mandal and S. Kumar, *J. Chem. Phys.* **139**, 165101 (2013).
- ³⁷M. P. Allen and D. J. Tildesley, *Computer Simulation of Liquids* (Oxford Science, Oxford, UK,) (1987).
- ³⁸D. Frenkel and B. Smit, *Understanding Molecular Simulation* (Academic Press UK) (2002).
- ³⁹P. G. de Gennes, *Scaling Concepts in Polymer Physics* (Cornell University Press, Ithaca) (1979), S. Kumar and Y. Singh, *Phys. Rev. E* **48**, 734 (1993).
- ⁴⁰For a chain of 16 base-pairs, the rupture force (f_c) and the melting temperature (T_m) are ~ 16 and ~ 0.181 respectively. Whereas for 12 base-pairs, their values are ~ 12 and ~ 0.171 , respectively.
- ⁴¹M. S. Li *Biophys. J.* **93**, 2644 (2007).
- ⁴²M. S. Li and M. Cieplak, *Phys. Rev E* **59**, 970 (1999).
- ⁴³J. SantaLucia Jr. and D. Hicks, *Annul. Rev. Biophys. Biomol. Struct* **33** 415 (2004).
- ⁴⁴S. Srivastava and N. Singh, *J. Chem. Phys.* **134**, 115102 (2011).
- ⁴⁵Following relations may be used to convert dimensionless units to real units: $T = \frac{k_B T^*}{\epsilon}$, $t^* = (\frac{m\sigma^2}{\epsilon})^{\frac{1}{2}} t$ and $r = \frac{r^* \sigma}{\epsilon}$, where T^* , t^* , r^* , and ϵ are temperature, time, distance, and characteristic hydrogen bond energy in real units, respectively. σ is the inter-particle distance at which the potential approaches to zero. Now, if one sets effective base pairing energy $\epsilon \sim 0.17$ eV, which is obtained by comparing the melting temperature in the reduced $T_m (= 0.161)$ to the one obtained from the oligo-calculator⁴⁶ for the same sequence, one

gets $T_m \approx 56^\circ C$. By setting average mass of each bead $\approx 5 \times 10^{-22}g$ and $\sigma = 5.17\text{\AA}$, one can obtain relation between real time t^* and reduced time t as $t^* \sim 3t$ ps.

⁴⁶W. A. Kibbe, *Nucleic Acids Res.* **35**, W43 (2007).

⁴⁷P. G. de Gennes, *C. R. Acad. Sci. Paris* **2**, 1505 (2001).

⁴⁸This approximate value can be obtained by putting different elastic constants involved in the expression of χ^{-1} . In the present simulation, we have used $k = Q$ (=100) i.e. the spring constant associated with the covalent bonds along the backbone of the chain. The spring constant R associated with the base-pairs has been obtained by expanding the LJ potential around its equilibrium value and setting it equal to zero above the cut off distance, where rupture takes place. The second (harmonic) term of the expansion gives the elastic constant $R \sim 0.5$ associated with the LJ potential involved in the base-pairing.

⁴⁹M. Santosh and P. K. Maiti, *J. Phys.: Condens. Matter* **21**, 034113 (2009).

⁵⁰<http://structure.usc.edu/make-na/server.html>.

⁵¹W. L. Jorgensen, J. Chandrasekhar, J. D. Madura, R. W. Impey, and M. L. Klein, *J. Chem. Phys.* **79** (1983).

⁵²We have used the constant force routine developed by P. K. Maiti and his group.

⁵³T. Darden, D. York and L. J. Pedersen, *Chem. Phys.* **98**, 10089 (1993).

⁵⁴U. Essmann, L. Perera, M. L. Berkowitz, T. Darden, H. Lee and L. G. Pedersen, *J. Chem. Phys.* **103**, 8577 (1995).

⁵⁵P. K. Maiti, T. A. Pascal, N. Vaidehi and W. A. Goddard III, *Nucleic Acids Res.* **32**, 6047 (2004).

⁵⁶P. K. Maiti and B. Bagchi, *Nano Lett.* **6**, 2478 (2006).

⁵⁷Here, the simulation time is about $7ns$, and hence rupture force is found to be one order higher than AFM.